Processing Temperature and Surface Na Content of TiO2 Nanocrystallites in Films for Solid-State Dye-Sensitized Solar Cells

ARTICLE *in* THE JOURNAL OF PHYSICAL CHEMISTRY C · NOVEMBER 2010

Impact Factor: 4.77 · DOI: 10.1021/jp1063676

7 AUTHORS, INCLUDING:

Dominic Lingenfelser
Bosch GmbH
10 PUBLICATIONS **29** CITATIONS
SEE PROFILE

Barbara Völker
Bosch GmbH
3 PUBLICATIONS **16** CITATIONS
SEE PROFILE

Thomas Mayer
Technical University Darmstadt
94 PUBLICATIONS **1,102** CITATIONS
SEE PROFILE

Processing Temperature and Surface Na Content of TiO_2 Nanocrystallites in Films for Solid-State Dye-Sensitized Solar Cells

Xianjin Feng,[†] René Hock,[†] Eric Mankel,[†] Dominic Lingenfelser,[‡] Barbara Völker,[‡] Thomas Mayer,*[,†] and Wolfram Jaegermann[†]

Institute of Materials Science, Darmstadt University of Technology, D-64287 Darmstadt, Germany, and Institute of Physical Chemistry, University of Heidelberg, D-69120 Heidelberg, Germany

Received: July 9, 2010; Revised Manuscript Received: October 12, 2010

We investigate changes of the chemical surface composition of nanocrystalline TiO_2 films induced by systematic temperature variations. Two heating procedures in air are investigated: a hot plate, in similarity to sintering, and an air heating gun, in similarity to activation before staining. Stepwise heated samples have been analyzed at room temperature using synchrotron induced photoelectron spectroscopy and X-ray photoelectron spectroscopy. With increasing temperature, the samples show increasing photoemission of Na-related orbitals. To identify the source of the surface Na—either the soda lime glass substrate or the TiO_2 powder itself—we investigate TiO_2 films sintered on a Si substrate and films produced from TiO_2 powders containing Na from <10 to 170 ppm. Clearly, the TiO_2 powder itself is identified as the source of the temperature-enriched Na on the TiO_2 crystallites' surfaces. Efficiency measurements on SDSCs sorted by the Na bulk content corroborate the importance of the Na content for the cell efficiency.

1. Introduction

There is much interest in dye-sensitized solar cells (DSSCs) due to their low cost and reasonably high efficiency, which make them a potential alternative to the conventional silicon solar cells.[1−3] Solar energy conversion efficiencies of up to 11% have been achieved in DSSCs using liquid electrolytes.[4,5] However, the use of liquid electrolytes leads to several practical problems, such as solvent evaporation due to seal imperfection causing degradation.[6,7] Therefore, the solid-state dye-sensitized solar cells (SDSCs), in which liquid electrolytes are replaced by organic hole conductors, become promising.[8] A typical SDSC consists of several different material layers: optically transparent front electrodes, such as fluorine-doped tin oxide (FTO); a compact TiO_2 layer blocking direct interaction of FTO and the hole conductor; a dye adsorbed on mesoporous nanocrystalline (nc) TiO_2 as an absorber and a photoelectron transporting layer; a solid organic or inorganic hole-transport layer (HTL) rereducing the dye after electron injection into the TiO_2 photoanode; and a gold back contact.[9]

Efforts are made on synthesizing novel dyes and hole conductors[10,11] to improve the efficiency of SDSCs, but less attention has been paid to the analysis and precise control of TiO_2 processing parameters. However, using the same materials and seemingly the same protocol, films prepared at different laboratories lead to varied efficiencies, indicating uncontrolled processing variations. TiO_2 nanocrystalline films used as the photoanode of DSSCs and SDSCs are usually exposed to heat treatment in the temperature range of 450−550 °C during sintering. Either the sintered films are put still warm from sintering into the dye solution or samples stored at RT are activated by heat treatment just before dye staining.[12,13] Therefore, in the present study, the effect of ex situ heat treatment on the chemical composition of nc TiO_2 films was investigated using photoelectron spectroscopy. Photoelectron spectroscopy, especially when induced by synchrotron radiation, is, in general, a powerful tool to characterize chemical and electronic surface properties, which are of utmost importance for nc TiO_2 films due to the nanostructured morphology. In previous measurements, we concentrated on the analysis of the chemical and electronic structure of DSSCs. SXPS measurements on in situ prepared TiO_2 by CVD to ex situ sintered films proved that the chemical and electronic structure can be well compared even when measuring with the highest surface sensitivity. In previous work,[14] we found that the TiO_2 gap state distribution is varied, specifically, dependent on the electrolyte solvent adsorbed. Further, we found that the solvent acetonitrile separates the N_3 Ru dye molecules from each other and induces a beneficial alignment of the dye charge-transfer vector normal to the TiO_2 surface.[15] Here, we concentrate on the chemical variations induced by ex situ temperature treatment on ex situ sintered nc TiO_2 photoelectrodes for SDSCs. A clear correlation is found between heating temperature and surface enriching of Na. As the source of the surface Na, clearly, the TiO_2 powder itself is evidenced.

2. Experimental Procedure

Different ex situ sintered TiO_2 nc samples were provided by our project partners, BOSCH Company, from Germany, and, EPFL, from Switzerland, using anatase TiO_2 powder from different commercial sources. Thin films of the TiO_2 blocking layer were deposited onto the FTO conducting glass by spray pyrolysis at 450 °C. Nanocrystalline TiO_2 films were then prepared on the compact TiO_2 blocking layer by spreading the paste made from different batches of TiO_2 powders using screen printing, followed by sintering at nominally 450 °C. On Si wafer substrates, nc TiO_2 films were directly deposited onto the oxide covered Si(111) wafer surface using the same procedure. The as-received samples were heated ex situ in air by a hot plate or using an air heating gun and transferred rapidly into the UHV

* To whom correspondence should be addressed. Tel: +49 6151 165532. Fax: +49 6151 166308. E-mail: mayerth@surface.tu-darmstadt.de.
[†] Darmstadt University of Technology.
[‡] University of Heidelberg.

10.1021/jp1063676
Published on Web 11/04/2010

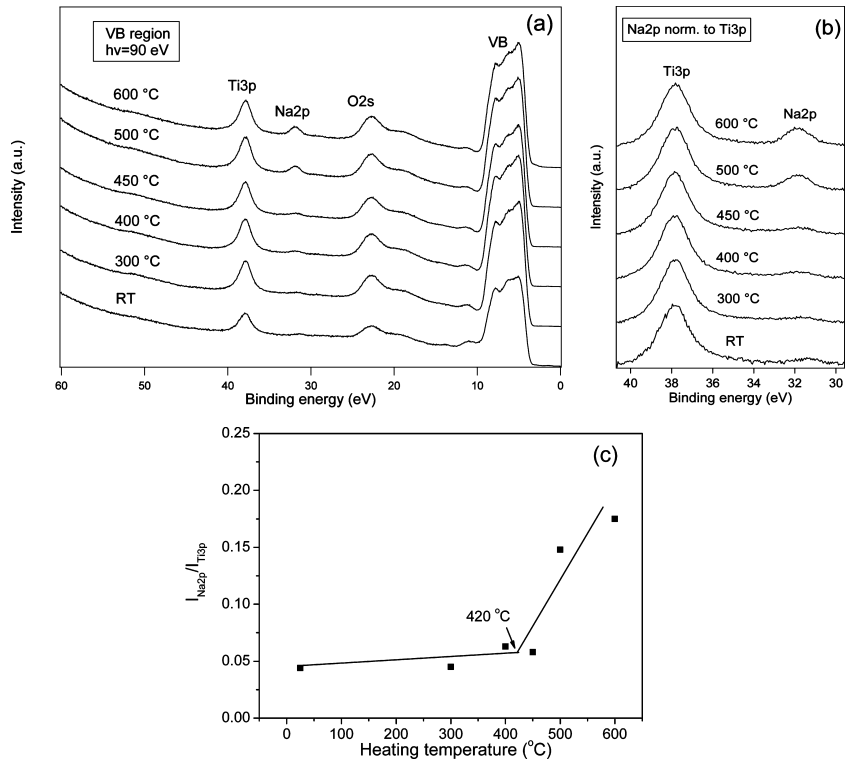

Figure 1. SXPS spectra of the nc TiO_2 film in the course of hot plate heat treatment taken at $h\nu = 90$ eV: (a) VB region normalized to the beam current and (b) Na 2p emission normalized to the Ti 3p intensity. (c) Plot of the intensity ratio of Na 2p to Ti 3p. As a guide to the eye, two straight lines are drawn through the data points.

chamber via a load lock. The temperature was varied stepwise in the range of 300−600 °C and kept constant for 30 min at each step. The temperature was measured using a thermocouple pressed to the TiO_2 film of the sample.

SXPS experiments were performed at beamlines TGM7 and U49/PGM2 of the BESSY storage ring in Berlin using our experimental station SoLiAS, dedicated to solid−liquid interface analysis.[16] The base pressure of the analysis chamber was in the 10^{-10} mbar range. The binding energies of all spectra were referenced to the Fermi level of a sputter-cleaned gold test sample. Intensities of the spectra were normalized to the current of the electron storage ring. The XPS study was carried out in the Darmstadt Integrated System for Solar Research (DAISYSOL)[17] by using an ESCALAB 250 spectrometer equipped with a monochromated Al Kα X-ray source ($h\nu = 1486.6$ eV). Binding energies were calibrated with sputter-cleaned Ag samples by setting the Ag 3d binding energy to 386.27 eV. The overall energy resolution for Al Kα excited photoelectron spectra was better than 400 meV, and the base pressure of the system was below 10^{-9} mbar.

For the efficiency measurements, SDSCs have been prepared using stored TiO_2 electrodes without and with heat treatment for 15 min at 150 °C in an oven just before dye staining. A detailed description of cell preparation will be given elsewhere. The SDSCs consist of commercial FTO on glass (Hartford TEC 15), a 50 nm TiO_2 blocking layer produced by spray pyrolysis of diisopropoxytitanium bis(acetylacetonate), a 1.9 μm nanoporous TiO_2 film that was screen-printed and sintered for 30 min at 450 °C, the dye, the organic hole conductor, spiro-MeOTAD, and a Ag back contact. For the measurement of illuminated $I-V$ curves, a solar simulator of AM 1.5 (1 sun) and a 0.1 gray filter (0.1 sun) were used.

3. Results and Discussion

To simulate the sintering process performed during the preparation of nc TiO_2 films, a series of heat treatments were carried out on the TiO_2 nc film with the FTO substrate using a hot plate. SXPS spectra of the valence band (VB) region, including the oxygen 2p dominated valence band between 3.6 and 9.9 eV, the O 2s emission at the 22.8 eV peak position, and the Ti 3p shallow core level at 37.9 eV taken with 90 eV photon energy, are displayed in Figure 1a in the course of stepwise increasing temperature starting with the nonheated sample at RT up to 600 °C. The spectrum of the nontreated sample coincides with spectra taken on ex situ prepared samples, as published before.[15] Already for the nontreated sample, a small emission at about 31.6 eV can be observed when the spectra are normalized to the intensity of the substrate Ti 3p emission, as displayed in Figure 1b. A clear increase of this emission is observed in the spectrum measured after tempering at 500 °C. The binding energy of this emission suggests the assignment to the 2p orbital of Na^+ cations, as observed for Na^+ ions on WSe_2.[18] Literature values for the 2p binding energy of metallic Na are given with 30.6 eV.[18,19] The intensity ratio of Na 2p to Ti 3p core levels as a function of heating temperature is displayed in Figure 1c. As the cross-section ratio for the Na 2p to Ti 3p emission is 4.4, the integrated emission translates to formal Na layer thicknesses of 0.05 Å at RT and to 0.20 Å at 600 °C, as calculated from formula (3) in the Appendix. An activation temperature around 420 °C may be read from Figure 1c.

Stepwise heat treatments using an air heating gun were also performed on the same kind of sample to simulate the heat treatment before dye staining. SXPS spectra of the VB region taken at $h\nu = 90$ eV are shown in Figure 2a. The Na 2p level is already observed at RT besides the Ti 3p and O 2s shallow

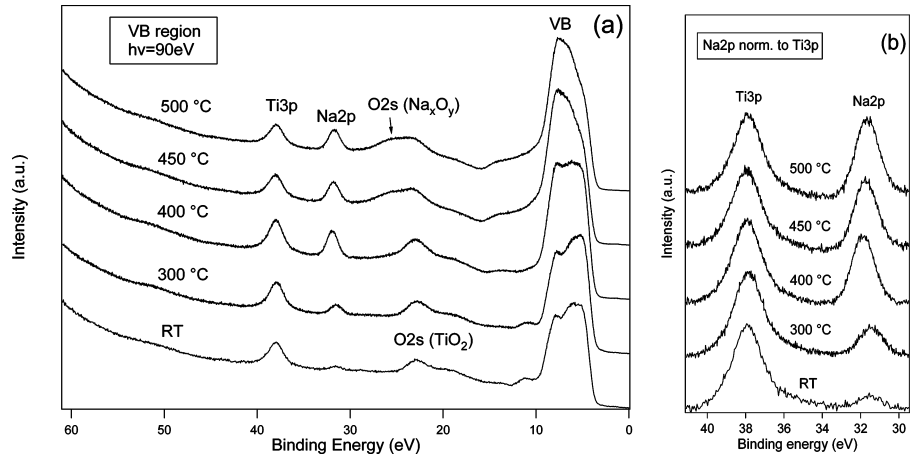

Figure 2. SXPS spectra of (a) the VB region normalized to the beam current and (b) the Na 2p core level normalized to the intensity of the Ti 3p core orbital taken at $h\nu = 90$ eV for the nc TiO_2 film with heat treatment using an air heating gun.

core levels. After heat treatment, the intensity of the Na 2p core level increases obviously, which can be more clearly observed when the spectra are normalized to the intensity of the substrate Ti 3p emission, as displayed in Figure 2b. At 450 °C, additional changes are observed in both the O 2s core level and the valence band. A phase transition of TiO_2 from anatase to rutile was first suspected as the cause of the change of the VB spectra, and Raman measurements were performed as a test. However, only the anatase phase was observed also for the 500 °C heated sample, indicating that no phase transition of bulk TiO_2 occurred. For the O 2s core level, a higher binding energy component arises, indicating the formation of a new oxide. A similar valence band structure was also reported by our group on the study of Na deposition on V_2O_5 films[20,21] and identified as Na_xO_y. Therefore, the changes in the O 2s core level and the valence band at high temperature are ascribed to the formation of Na_xO_y. As the formation of the sodium oxide is not observed by heating with the hot plate, we assume that additional activation of oxygen is necessary to induce the reaction with the Na^+ ion. This activation may be induced by the hot Kanthal wire heater spiral of the air heating gun, which appears yellow-reddish, indicating a temperature well above 1000 °C. The sample is heated by a flow of hot air. The air is heated by passing the heater spiral, and oxygen-containing species may, in part, be modified, for example, ionized by capture of thermionic emitted electrons or catalytically decomposed similar to the technological process of hot wire activated chemical vapor deposition (HWCVD).[22] In contrast, using the hot plate, the sample is heated by a heater spiral through a glass ceramic plate with the plate temperature set to 500−600 °C. The formal Na layer thickness calculated using formula (3) increases from 0.12 at RT to 0.77 Å at 600 °C.

To further confirm that the emission at 31.6 eV is due to Na, an nc TiO_2 sample with a high Na content was also measured with XPS before and after heat treatment at 600 °C using a hot plate, as shown in Figure 3. In addition to the emission at 31.6 eV, an emission at 1072.5 eV, which is clearly due to the Na 1s core level, increases with temperature.

As the mobility of Na ions in both glass[23−25] and TiO_2[26−28] is well-known, the soda lime glass substrate or Na contaminations in the TiO_2 powder itself are possible sources for the temperature-enriched surface Na. To identify the Na source, a series of heat treatments using both a hot plate and an air heating gun were performed on an nc TiO_2 film prepared on a Si(111) wafer substrate. The SXPS spectra of the VB region normalized to the beam current are shown in Figure 4a. Again, the Na 2p

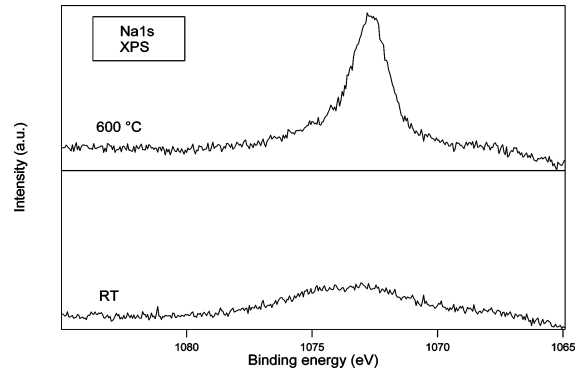

Figure 3. XP spectra of the Na 1s core level for a sample with a high Na content at RT and heated to 600 °C using a hot plate (same sample for which SXPS results are shown in Figure 6).

emission increases after heating with the hot plate as well as with the air heating gun. As on the FTO-covered glass substrate, besides the appearance of the Na 2p emission, no obvious changes are induced with the hot plate, but additional changes in the O 2s shallow core level and the valence band are induced with the air heating gun. The change of the Na 2p core level can be more clearly seen in the normalized spectra in Figure 4b. For the 400 and 600 °C hot plate heated samples, charging effects occurred during the measurements and the spectra were adjusted in binding energy for better comparison. Thus, the small change in the energetic distance between Ti 3p and Na 2p might be an artifact rather than a chemical core-level shift. Because the influence of the Na-contained glass substrate is excluded, the SXPS results shown in Figure 4 indicate that the Na content observed at the surface of TiO_2 is related to the Na contained in the TiO_2 powder used for sintering.

To investigate the correlation between bulk and surface Na contents, several as-is nc TiO_2 films prepared from TiO_2 powders with known upper limits of Na contents were measured. The Na content of TiO_2 powders was determined by inductively coupled plasma optical emission spectroscopy (ICP-OES), a method that determines the bulk elemental composition. In general, for example, in the sol−gel synthesis of TiO_2 nanoparticles, structure-directing agents, for example, sodium dodecyl sulfate, are used.[29] The variation of the Na content is due to variations in the respective synthesis and purification parameters. The SXPS spectra of the Na 2p core level normalized to the intensity of the Ti 3p core orbital are shown in Figure 5a, from which it can be seen that the intensity of the Na 2p emission

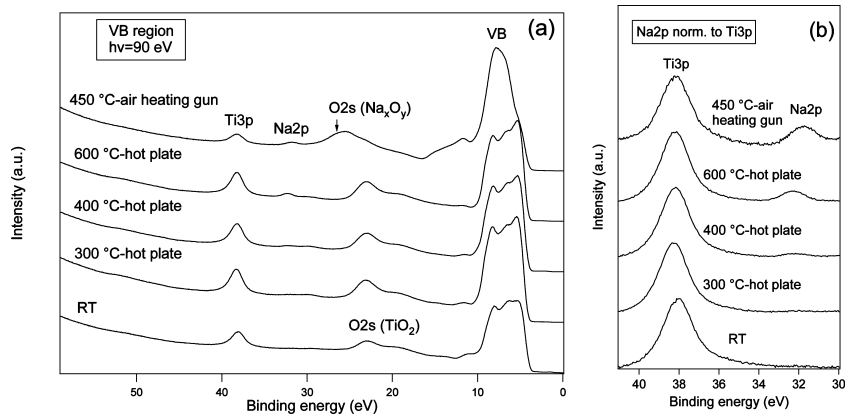

Figure 4. SXPS spectra taken at $h\nu = 90$ eV for the nc TiO_2 film prepared on Si(111) as a result of heat treatment with a hot plate and an air heating gun: (a) VB region normalized to the beam current and (b) Na 2p core level normalized to the intensity of Ti 3p.

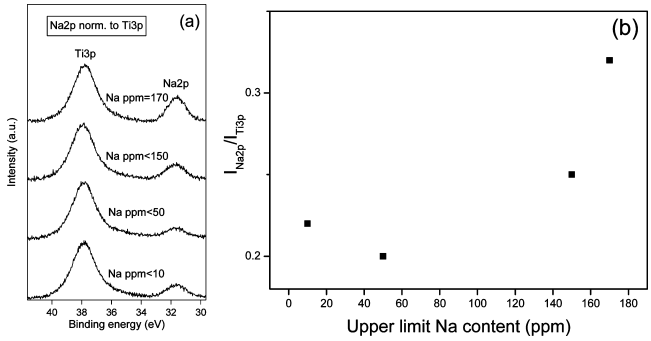

Figure 5. (a) SXPS spectra of Ti 3p and Na 2p shallow core levels for nc TiO_2 films sintered using powders with different Na contents as indicated. The spectra are taken at $h\nu = 90$ eV and normalized to the intensity of Ti 3p. (b) Plot of the intensity ratio of Na 2p to Ti 3p versus the upper limit of the Na content.

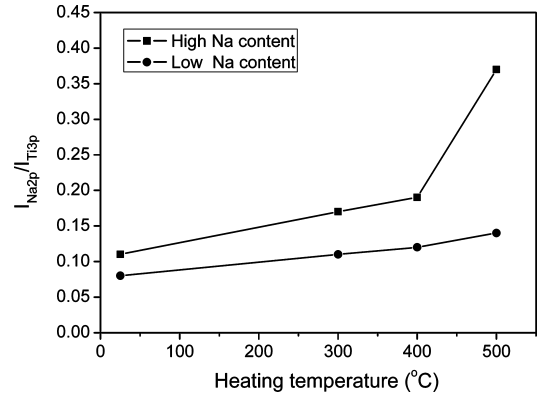

Figure 6. Intensity ratio of Na 2p to Ti 3p core levels as a function of heating temperature for nc TiO_2 films prepared from TiO_2 powder with high and low Na contents, respectively.

correlates to some extent to the Na content in the TiO_2 powder. Such a correlation is more clearly seen when plotting the intensity ratio of the Na 2p to the Ti 3p emission as a function of the upper limit of the Na content determined for the TiO_2 powder used for sintering of the film (Figure 5b).

To further investigate the effect of the Na content in the TiO_2 powder on the intensity increase of the Na 2p core level with temperature, two samples prepared on FTO from TiO_2 powders with high and low Na contents are compared. The intensity ratio of Na 2p to Ti 3p core levels as a result of hot plate heating is displayed in Figure 6. As the heating temperature increases, the intensity increase of Na 2p for the sample prepared from TiO_2 powder with a high Na content is much more obvious than that with a low Na content, which corroborates that the temperature-increased surface Na content is due to the Na content in the TiO_2 powder.

Interestingly, when the TiO_2 films are annealed using the hot plate, the Na 2p emission increases while no other features of the TiO_2 spectra change. Especially, the valence band, which is very sensitive to structural and chemical changes, is not altered. Only when the air heating gun is used are changes of the valence band observed. Therefore, we believe that, using the hot plate, the Na^+ ions migrate from the bulk of the respective TiO_2 crystallite toward its surface but do not transmit the surface. We propose a stabilized subsurface configuration for Na^+ ions in analogy to the stabilized subsurface Ti interstitial, as calculated by Wendt et al.[30] Before heat treatment, the Na^+ ions are randomly distributed in the bulk of the TiO_2 crystallites. The heat treatment with a hot plate results in the migration of Na^+ ions from the bulk of the TiO_2 nanoparticles to subsurface sites, where they are stabilized. Using an air heating gun at high temperature, Na^+ ions transmit the TiO_2 surface, reacting with activated oxygen from the air heating gun. A sketch of the Na distribution for the respective treatments is given in Figure 7.

As for dye-sensitized solar cells, the TiO_2 surface is very large and directly involved in chemical anchoring of the dye, electron transfer from the dye LUMO to the TiO_2 conduction band, and recombination of electrons in TiO_2 with holes in the dye HOMO.[31] The efficiency is extremely sensitive to chemical and electronic surface variations; that is, the surface and subsurface Na contents are expected to influence strongly the performance of the solar cell. Surface gap states are widely thought to play an important role in the electron-transport and recombination processes.[14,32,33] Therefore, we checked carefully the surface gap state distribution using resonant photoemission. No clear correlation between the intensity of the gap states and the surface Na content was found. In Figure 8, we present efficiency measurements on SDSCs with an area of 20 mm^2 at 1/10 and 1 sun illumination from a solar simulator sorted by the Na bulk content of the TiO_2 electrodes before and after annealing at 150 °C for 15 min in air for (a) the standard metal-free indoline dye D102[34] and (b) a modified dye from BASF. Up to around 150 ppm Na, all samples at both intensities and for both dyes show an efficiency increase with annealing of the TiO_2 electrodes, which is caused by increased dye adsorption due to OH desorption from the TiO_2 surface. At 170 ppm Na, D102 shows a decrease at 1/10 sun, whereas at 1 sun, the efficiency does not change. With the "BASF dye", at both intensities, a decrease after the heat treatment is measured, which is stronger

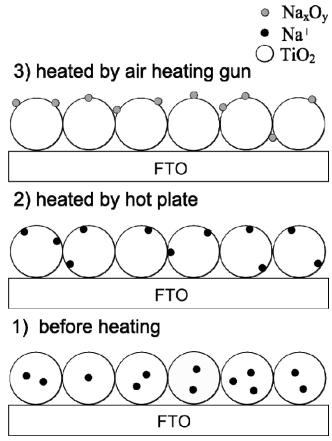

Figure 7. Sketch of the Na distribution for the indicated heat treatments.

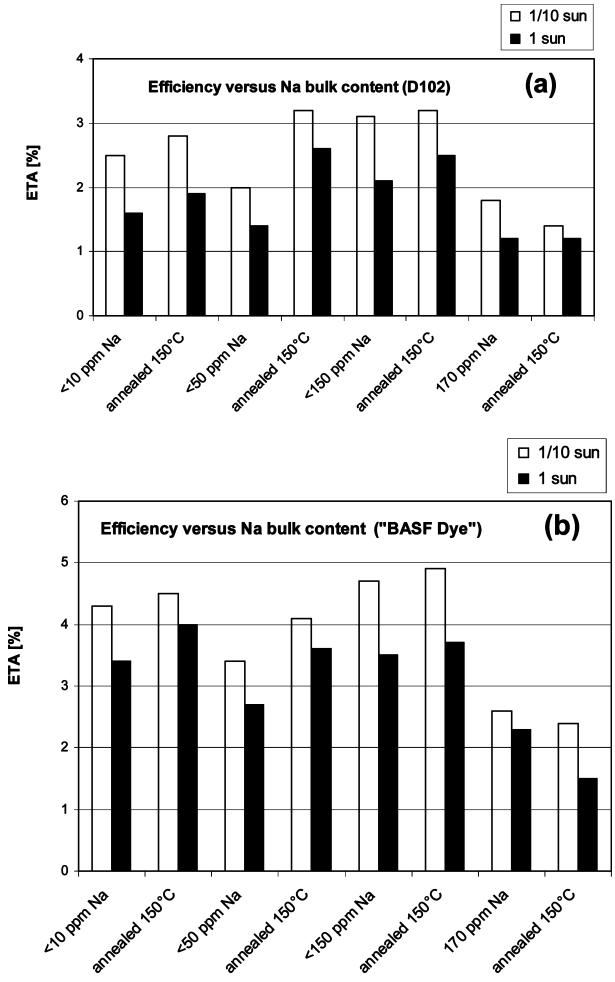

Figure 8. Efficiency measurements of SDSCs sorted according to the Na bulk content of the TiO_2 electrode for two intensities before and after heat treatment at 150 °C before dye staining for the (a) indoline dye D102 and (b) "BASF dye".

at the higher intensity. According to our SXPS measurements (see Figures 1 and 6), only minor changes of the surface Na content are expected at 150 °C. The sorting of efficiency measurements according to the Na bulk content, as displayed in Figure 8, gives some indication that the efficiency could be influenced by the surface Na content that varies dependent on the bulk content. There is also some indication that an optimum Na concentration may be given for the respective dye used. Further efficiency measurements using TiO_2 with deliberately varied Na content and varied heat treatments are needed to differentiate the role of surface Na in SDSCs.

4. Conclusions

Systematic ex situ heat treatments using a hot plate and an air heating gun have been performed on different ex situ prepared nc TiO_2 films. In both cases, the intensity of the Na 2p core level increases after heat treatment. The Na 2p binding energy indicates that Na is in the 1+ ionic state. Compared with heat treatments with the hot plate, the increase of Na 2p for heat treatments using an air heating gun is more obvious, and additional changes in both the O 2s shallow core level and the valence band are observed above 450 °C, which we assign to the formation of Na_xO_y on top of the TiO_2 crystallites' surfaces. As also on the Si substrate, the temperature-driven increase of the surface Na content is observed, we pinpoint TiO_2 powder itself as the source of the surface Na content. The higher the Na content of the TiO_2 powder, the more obviously the Na 2p peak increases with temperature. In conclusion, we propose that variations in surface Na content, distribution, and chemical composition due to variations in temperature treatment are the possible causes of different efficiencies of SDSCs prepared from the same materials at different laboratories. Efficiency measurements on SDSCs using TiO_2 with different bulk Na contents and heat treatment at 150 °C corroborate the conclusion that surface Na could influence the cell performance.

Acknowledgment. This work is funded within the OPEG 2010 initiative by the German Federal Ministry of Research and Technology as a cooperation with the BOSCH Company as an industry partner. The authors also thank the other members of EPFL and BESSY.

Appendix

For a homogeneous overlayer on a substrate, the photoemission intensity of the overlayer and the substrate is given by

$$I_o = I_o^\infty\left[1 - \exp\left(\frac{-d}{\lambda_a^o \cos\theta}\right)\right] \quad \text{and} \tag{1}$$

$$I_s = I_s^\infty \exp\left(\frac{-d}{\lambda_a^s \cos\theta}\right) \tag{2}$$

where I_o^∞ and I_s^∞ are intensities (i.e., peak areas) for the overlayer of infinite thickness and the clean substrate; d is the thickness of the overlayer; λ_a^o and λ_a^s are the mean free path for photoelectrons, which are generated in the overlayer and the substrate, traversing the overlayer; and θ is the angle between the analyzer and the sample surface normal. For Na 2p and Ti 3p, we approximate

$$\lambda_a^o = \lambda_a^s = \lambda, \quad d = \ln\left(\frac{I_o I_s^\infty}{I_s I_o^\infty} + 1\right)\lambda\cos\theta = \ln\left(\frac{I_o I_s^\infty/\sigma_o\sigma_s}{I_s I_o^\infty/\sigma_o\sigma_s} + 1\right)\lambda\cos\theta = \ln\left(\frac{I_o/\sigma_o}{I_s/\sigma_s} + 1\right)\lambda \tag{3}$$

(given $\cos\theta = 1$ in our experiment and $[(I_s^\infty/\sigma_s)/(I_o^\infty/\sigma_o)] = 1$ by definition, where σ_o and σ_s are cross sections for the respective overlayer and substrate orbital). The approximate values of λ,

$\sigma_{Na\ 2p}$, and $\sigma_{Ti\ 3p}$ at $h\nu = 90$ eV are 5 Å, 5.5 Mb, and 1.25 Mb, respectively.[35]

References and Notes

(1) O'Regan, B.; Grätzel, M. *Nature* **1991**, *335*, 737.
(2) Hagfeldt, A.; Grätzel, M. *Chem. Rev.* **1995**, *95*, 49.
(3) McConnell, R. D. *Renewable Sustainable Energy Rev.* **2002**, *6*, 273.
(4) Grätzel, M. *J. Photochem. Photobiol., A* **2004**, *164*, 3.
(5) Grätzel, M. *Inorg. Chem.* **2005**, *44*, 6841.
(6) Tennakone, K.; Kumara, G.; Kottegoda, I. R. M.; Perera, V. P. S. *Chem. Commun.* **1999**, 15.
(7) Wu, J.; Lan, Z.; Lin, J.; Huang, M.; Hao, S.; Sato, T.; Yin, S. *Adv. Mater.* **2007**, *19*, 4006.
(8) Grätzel, M. *Nature* **2001**, *414*, 338.
(9) Karthikeyan, C. S.; Thelakkat, M. *Inorg. Chim. Acta* **2008**, *361*, 635.
(10) Cervini, R.; Cheng, Y. B.; Simon, G. *J. Phys. D: Appl. Phys.* **2004**, *37*, 13.
(11) Ravirajan, P.; Haque, S. A.; Durrant, J. R.; Poplavskyy, D.; Bradley, D. D. C.; Nelson, J. *J. Appl. Phys.* **2004**, *95*, 1473.
(12) Meng, Q. B.; Takahashi, K.; Zhang, X. T.; Sutanto, I.; Rao, T. N.; Sato, O.; Fujishima, A.; Watanabe, H.; Nakamori, T.; Uragami, M. *Langmuir* **2003**, *19*, 3572.
(13) Taguchi, T.; Zhang, X. T.; Sutanto, I.; Tokuhiro, K.; Rao, T. N.; Watanabe, H.; Nakamori, T.; Uragami, M.; Fujishima, A. *Chem. Commun.* **2003**, 2480.
(14) Schwanitz, K.; Weiler, U.; Hunger, R.; Mayer, T.; Jaegermann, W. *J. Phys. Chem. C* **2007**, *111*, 849.
(15) Schwanitz, K.; Mankel, E.; Hunger, R.; Mayer, T.; Jaegermann, W. *Chimia* **2007**, *61*, 796.
(16) Mayer, T.; Lebedev, M.; Hunger, R.; Jaegermann, W. *Appl. Surf. Sci.* **2005**, *252*, 31.
(17) Fritsche, J.; Klein, A.; Jaegermann, W. *Adv. Eng. Mater.* **2005**, *7*, 914.
(18) Mayer, T.; Lehmann, J.; Pettenkofer, C.; Jaegermann, W. *Chem. Phys. Lett.* **1992**, *198*, 621.
(19) Andersen, J. N.; Lundgren, E.; Nyholm, R.; Qvarford, M. *Surf. Sci.* **1993**, *289*, 307.
(20) Wu, Q. H.; Thissen, A.; Jaegermann, W. *Solid State Ionics* **2004**, *167*, 155.
(21) Wu, Q. H.; Thissen, A.; Jaegermann, W. *Appl. Surf. Sci.* **2005**, *252*, 1801.
(22) Abrutis, A.; Plausinaitiene, V.; Skapas, M.; Wiemer, C.; Gawelda, W.; Siegel, J.; Rushworth, S. *J. Cryst. Growth* **2009**, *311*, 362.
(23) Hunger, R.; Schulmeyer, T.; Klein, A.; Jaegermann, W.; Lebedev, M. V.; Sakurai, K.; Niki, S. *Thin Solid Films* **2005**, *480*, 218.
(24) Lim, C.; Day, D. E. *J. Am. Ceram. Soc.* **1977**, *60*, 473.
(25) Njiokep, E. M. T.; Mehrer, H. *Solid State Ionics* **2006**, *177*, 2839.
(26) Benyamin, K. *Solid State Ionics* **1994**, *73*, 303.
(27) Mattsson, M. S.; Niklasson, G. A.; Granqvist, C. G. *J. Appl. Phys.* **1997**, *81*, 2167.
(28) Lunell, S.; Stashans, A.; Ojamäe, L.; Lindström, H.; Hagfeldt, A. *J. Am. Chem. Soc.* **1997**, *119*, 7374.
(29) Liao, D. L.; Liao, B. Q. *J. Photochem. Photobiol., A* **2007**, *187*, 363.
(30) Wendt, S.; Sprunger, P. T.; Lira, E.; Madsen, G. K. H.; Li, Z. S.; Hansen, J. O.; Matthiesen, J.; Blekinge-Rasmussen, A.; Lægsgaard, E.; Hammer, B.; Besenbacher, F. *Science* **2008**, *320*, 1755.
(31) Shklover, V.; Ovchinnikov, Y. E.; Braginsky, L. S.; Zakeeruddin, S. M.; Grätzel, M. *Chem. Mater.* **1998**, *10*, 2533.
(32) Gregg, B. A. *Coord. Chem. Rev.* **2004**, *248*, 1215.
(33) Zhu, K.; Kopidakis, N.; Neale, N. R.; van de Lagemaat, J.; Frank, A. J. *J. Phys. Chem. B* **2006**, *110*, 25174.
(34) Schmidt-Mende, L.; Bach, U.; Humphry-Baker, R.; Horiuchi, T.; Miura, H.; Ito, S.; Uchida, S.; Grätzel, M. *Adv. Mater.* **2005**, *17*, 813.
(35) Yeh, J. J.; Lindau, I. *At. Data Nucl. Data Tables* **1985**, *32*, 1.

JP1063676